*RESEARCH ARTICLE*
*Eurasian J Bio Chem Sci, 6(1):31-40, 2023*
*https://doi.org/10.46239/ejbcs.1225044*

EJBCS

**Eurasian Journal of Biological and Chemical Sciences**

Journal homepage: www.dergipark.org.tr/ejbcs

# Molecular modeling and thermodynamics of the interaction between DNA base pairs and radon originated ionizing alpha radiation

**Caglar Celik Bayar***

*Zonguldak Bulent Ecevit University, Faculty of Engineering, Metallurgical and Materials Engineering Department, Zonguldak, Turkey

*Corresponding author : caglarbayar@gmail.com, caglarbayar@beun.edu.tr
Orcid No: https://orcid.org/0000-0002-2293-2963

Received : 27/12/2022
Accepted : 22/05/2023

**Abstract:** Ionizing alpha radiation ($He^{2+}$) is known to adversely affect human DNA, but the biochemical reasoning is not clear yet. Relatedly, the present computational study was conducted to investigate the effects of ionizing alpha radiation onto the Watson-Crick type DNA base pairs (nucleotides) Adenine-Thymine (AT') and Guanine-Cytosine (GC'). The long-range cation ($He^{2+}$)–π interactions were modeled for this purpose. A hybrid DFT functional of M06-2X was used with 6-31G(d,p) and 6-311G(d) basis sets at unrestricted level. The results showed that alpha radiation severely changed the considered base pairs' hydrogen bond lengths and their interaction enthalpies and Gibbs free energies, however, the more drastic changes were observed in GC' when compared to those of AT'. This observation was also supported with performed frontier molecular orbital analyses. GC' was more favored to form $He^{2+}$ complexes (oxidize) than AT' and consequently these complexes had more exothermic interaction energies (formed more spontaneously) than that of AT'. It could be highlighted that the molecular modeling proposed in this study would contribute to the enlightenment of the uncertainty in this field.

**Keywords:** DNA base pairs, alpha radiation, interaction enthalpy, interaction Gibbs free energy, M06-2X



## 1. Introduction

Radon gas ($^{222}Rn$) is the radiation source that is naturally produced in the soil and has the most ionizing effect with its alpha (α) radiation. The radioactive property of radon atoms and their being in gaseous state at the same time cause adverse effects on human health by being inhaled into the lungs. The most important negative effect is lung cancer. For the first time, Bale (Bale 1980) and Harley (Harley 1952) suggested that lung cancer does not arise directly from radon atoms, but from product nuclei formed by the decay of the radon atom (Soğukpınar 2013). The International Agency for Research on Cancer (IARC) defined radon gas as a cancer-causing agent in 1988. The risk of developing lung cancer in smokers who are exposed to 1-800 $Bq/m^3$ of radon gas has been reported 22-25 times higher than non-smokers. Both non-smokers and individuals who are not exposed to radon gas do not develop lung cancer (Soğukpınar 2013; Zeeb and Shannoun 2009).

Since radon gas is a member of the noble gas group, it is chemically passive and does not react. Since the half-life of radon gas is longer than the duration of inhalation (3,82 days), the radon gas that is inhaled is exhaled without decomposing again. Metal atoms ($^{214}Po$, $^{218}Po$, $^{214}Pb$ and $^{214}Bi$) are formed as a result of the decay of radon atoms. When these atoms adhere to airborne dust and aerosols and are inhaled into the lungs, they cling to the lung epithelium tissue surrounding the inner structure and are not expelled again during exhalation. The product formed by decomposition of radon, $^{214}Pb$, which has the longest half-life, decays in less than 27 minutes. Short-lived product nuclei degrade before the normal cleansing period of the lung, and may cause damage to sensitive epithelial cells and mutation in the DNA structure. The $^{214}Po$ and $^{218}Po$ nuclei, which have the highest decay energy, cause the greatest damage to the lung cells with α radiation they make. The very short half-life (55,6 s) of the thoron ($^{220}Rn$) atom, which is a second isotope of the radon atom, caused its density to be low in the environment under normal conditions. Likewise, actinon ($^{219}Rn$), a third radon isotope, has a very short half-life (3,96 s) and the relative abundance of the actinon main nucleus in nature is very low. For this reason, thoron and actinon are often neglected in radon gas measurements, and the $^{222}Rn$ isotope is generally referred to (Durrani and Ilić 1997; Soğukpınar 2013). The $^{222}Rn$ isotope is continuously produced in the natural decay series of element uranium ($^{238}U$). Therefore, radon gas-related lung cancer has been reported mostly in uranium miners in

the world. As people learn about the health effects of radon gas, the radon level in the mines is constantly monitored, and it is tried to be kept at a certain level with ventilation (Soğukpınar 2013).

The α-Particle cannot pass through human skin (National Radiological Protection Board 1998). However, when radioactive nuclei are degraded within the body through nutrition or breathing, they produce ionizing α-particles and can trigger different types of cancer. It was reported that ionizing alpha particles could cause chromosomal aberrations (Chen et al. 1984; Robertson et al. 2013), double strand DNA breaks and generate reactive oxygen species (Narayanan et al. 1997; Robertson et al. 2013) resulting in cell cycle shortening, apoptosis and an increased potential of carcinogenesis. Accordingly, the tumor suppressor gene TP53 (previously named p53) mutations and deletions were frequently observed in various cancers (Robertson et al. 2013; Wazer et al. 1994) including those of the lung and investigations previously located unique mutations in regions referred to as biomarkers (hotspots) that could result from radon exposure (Robertson et al. 2013). The related study was conducted on radon exposed 52 Colorado uranium miners having large and squamous lung cell carcinomas (Taylor et al. 1994). It was reported that 31% of the workers possessed the AGG to ATG (Arg→Met) transversions, at the TP53 gene, codon 249, exon 7. This result leaded the authors to highlight this region as a potential hotspot for radon associated lung cancer. However, no clear radon-induced TP53 hotspot mutations were identified in uranium miner cohorts in further studies (Hollstein et al. 1997; McDonald et al. 1995; Popp et al. 1999; Robertson et al. 2013; Wesch et al. 1999; Wiethege et al. 1999; Yang et al. 2000). Conclusively, it can be stated that the cellular and molecular carcinogenic effects of radon exposure are still complex and uncertain (Robertson et al. 2013).

The long-range interactions of electron-deficient alpha particle arising from radon decay and electron-rich DNA base pairs have not been enlightened in a molecular term up to now to the best of the knowledge. In the present study, possible long-range interactions were modelled between the alpha particle ($He^{2+}$ ion) and each of the ring of Watson-Crick type DNA base pairs, Adenine-Thymine (AT) and Guanine-Cytosine (GT), including π-bonds, separately. The considered DNA base pairs were neutral and consisted of 2'-deoxyribose-5'-phosphate residues which resembled the real case. However, they were not interacted with alpha particle because of the lack of π-bonds. The molecular modeling was performed using a hybrid DFT functional M06-2X suggested for noncovalent long-range interactions of main-group elements (Zhao and Truhlar 2008). Finally, comparisons were done between the alpha particle bound and non-bound DNA base pairs to find out the possible changes in hydrogen bond lengths and interaction Gibbs free energies. It was considered that such changes may cause serious damages in DNA structure and impair its vital functions. Since such an approach and possible interactions were not investigated before in the literature, this contributed the originality of the study.

## 2. Methods of Calculation

The structure optimizations and single point energy calculations including interaction enthalpies, interaction Gibbs free energies and frontier molecular orbital (FMO) analyses were performed in gas phase using Spartan 18 program software (Spartan'18 Parallel Suite 2018). A starting distance of 2.5Å between the alpha particle ($He^{2+}$ ion) and DNA base pair ring centres was used to aid in convergence and find the local minima on the potential energy surface. Initial interaction angles were chosen as $90^o$ in all complexes. The structure optimizations were performed at DFT UM06-2X/6-31G(d,p) level of theory (Zhao and Truhlar 2008) after performing the pre-optimizations at semi-empirical and Hartree-Fock levels. This basis set was previously applied to cation-π type interactions in the literature (Davis and Dougherty 2015; Dhindhwal and Sathyamurthy 2016). The interaction enthalpies, interaction Gibbs free energies and FMO energies of all the complexes were computed at UM06-2X/6-311(d)//UM06-2X/6-31(d,p) level of theory. The interaction enthalpies and Gibbs free energies were corrected considering basis set superposition error (BSSE) contributions (Ebrahimi et al. 2014; Mudedla et al. 2014). BSSE corrections use the Boys and Bernardi counterpoise technique (Boys and Bernardi 1970; Ebrahimi et al. 2014) which are due to overlap of the wave functions of the moieties (Mottishaw and Sun 2013). The calculations of all the considered complexes contained zero point energy corrections and had no imaginary frequencies which indicated that they stood for no transition states or saddle points on the potential energy surfaces.

## 3. Results and Discussion

### *3.1. Verifying the Basis Set Used*

Before interacting DNA base pairs with alpha particle, it was necessary to test the validity of DFT UM06-2X/6-31G(d,p) theoretical level for optimizations. For this purpose, X-ray experimental data for Watson-Crick type Adenine-Thymine (AT) and Guanine-Cytosine (GT) base pairs (without deoxyribose and phosphate rings) were used as reference values and data obtained from the theoretical calculations were compared with them. The optimized structures of the AT and GC base pairs were shown in Figure 1. The experimental and theoretical atomic distances involved in hydrogen bonding were listed in Table 1 for these base pairs. It was figured out that the calculated distance between N1-O1 atoms was the same as the experimental distance while N2-N3 distance was close to the experimental one for the AT base pair. On the other hand, the calculated O1-N4 distance was a bit shorter than the experimental value while N1-N3 distance was close to it for the GC base pair. The N2-O2 distance was obtained a bit longer but still close to the experimental distance for the same base pair. Experimental data existing in Table 1 were reported in the studies of Saenger (Saenger 1984) and Mo (Mo 2006), previously. AT base pair had two hydrogen bonds between H1-O1 and N2-H3 atoms while GC base pair had that of three between O1-H3, H1-N3 and H2-O2 atoms.

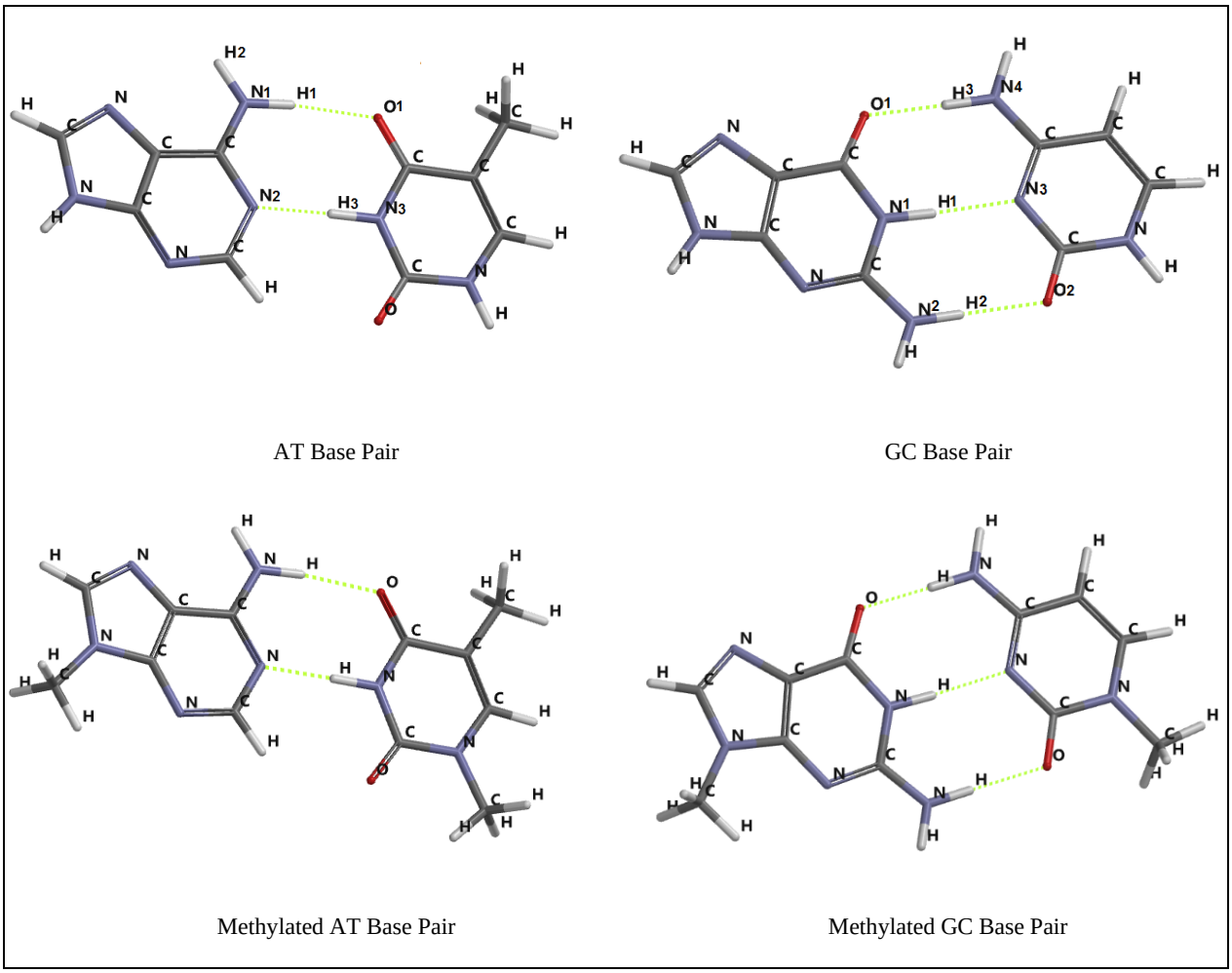


**Fig. 1** The optimized structures of Watson-Crick type Adenine-Thymine (AT), Guanine-Cytosine (GC), 9-methyladenine and 1-methylthymine (methylated AT), 9-methylguanine and 1-methylcytosine (methylated GC) base pairs at DFT UM06-2X/6-31G(d,p) theoretical level.

These hydrogen bond lengths ranged from 1.74 Å to 2.04 Å in the considered base pairs.

The experimental interaction enthalpies of the Watson-Crick type methylated base pairs, 9-methyladenine and 1-methylthymine (methylated AT) and 9-methylguanine and 1-methylcytosine (methylated GC), were also used to check out the validity of the theoretical level used in the present study. The experimental values were calculated at room temperature and reported as -12.1 kcal/mol for the methylated AT and -21.0 kcal/mol for the methylated GC base pairs, respectively (Brameld et al. 1997; Guerra et al. 2000; Yanson et al. 1979). Relatedly, close interaction enthalpies were calculated as -12.4 kcal/mol and -25.2 kcal/mol for the methylated AT and GC base pairs, respectively, in the study. The optimized structures of the considered methylated base pairs were also presented in Figure 1. It was possible to conclude that the calculated atomic distances showed almost no change for the methylated and unmethylated AT and GC species (Table 1). As a result, the theoretical and experimental comparison of the atomic distances and interaction enthalpies showed that the theoretical method used in the study was reliable.

### *3.2. Structure Optimizations, Hydrogen Bonds and Interaction Distances*

The optimized structures and aromatic ring numberings of Watson-Crick type AT and GC base pairs with 2'-deoxyribose-5'-phosphate residues (abbreviated as AT' and GC' throughout the study) were presented in Figure 2. These molecules were interacted with alpha particle and then optimized and thus formed the core of the study. Rings 1 and 2 belonged to the adenine side of AT' and guanine side of GC' whereas Ring 3 belonged to that of thymine and cytosine sides, respectively. The alpha particle had two possibilities to interact with these rings, from the upper and lower faces (Figure 2). The interactions from the upper faces were labeled as AT'-i and GC'-i (i=1-3), respectively, where i represented the aromatic ring numbers. Asterisk symbols ($^*$) over i, AT'-i$^*$ and GC'-i$^*$, were used to indicate the interactions from the lower face. In general, no significant shifts were observed at the end of the optimizations. However, there existed two exceptional optimized structures which were AT'-2$^*$ and AT'-(2-3)$^*$. The initial structure of AT'-1$^*$ ended up with AT'-2$^*$ in which the $He^{2+}$ ion shifted to the sterically less hindered side

**Table 1.** The atomic distances (Å) involved in hydrogen bonding of Watson-Crick type Adenine-Thymine (AT), 9-methyladenine and 1-methylthymine (methylated AT), Guanine-Cytosine (GC), 9-methylguanine and 1-methylcytosine (methylated GC) base pairs and AT'and GC' base pairs (with 2'-deoxyribose-5'-phosphate residues) and their $He^{2+}$ exposed derivatives calculated at DFT UM06-2X/6-31G(d,p) theoretical level. The interactions of $He^{2+}$ from the upper faces of the base pairs were denoted as AT'-i and GC'-i (i=1-3), respectively, where i represented the aromatic ring numbers. Asterisk symbols ($^*$) over i, AT'-i$^*$ and GC'-i$^*$, were used to indicate the interactions from the lower face (See Figure 2).

| | $N_1$-$O_1$ | $N_2$-$N_3$ | $H_1$-$O_1$ | $N_1$-$H_1$ | $N_2$-$H_3$ | $O_1$-$N_4$ | $N_1$-$N_3$ | $N_2$-$O_2$ | $O_1$-$H_3$ | $H_1$-$N_3$ | $H_2$-$O_2$ | $N_2$-$H_2$ |
|---|---|---|---|---|---|---|---|---|---|---|---|---|
| AT | 2.95 (2.95) | 2.79 (2.82) | 1.94 | | 1.74 | | | | | | | |
| Methylated AT | 2.94 | 2.80 | 1.93 | | 1.74 | | | | | | | |
| AT' | 2.94 | 2.79 | 1.92 | | 1.74 | | | | | | | |
| AT'-1 | 2.91 | 2.85 | | 1.92 | 1.82 | | | | | | | |
| AT'-2 | 2.92 | 2.85 | | 1.93 | 1.82 | | | | | | | |
| AT'-2$^*$ | 2.95 | 2.86 | | 1.96 | 1.83 | | | | | | | |
| AT'-(2-3)$^*$ | 2.91 | 2.84 | | 1.92 | 1.81 | | | | | | | |
| AT'-3 | 2.92 | 2.85 | | 1.93 | 1.82 | | | | | | | |
| AT'-3$^*$ | 2.92 | 2.85 | | 1.93 | 1.82 | | | | | | | |
| GC | | | | | | 2.79 (2.91) | 2.92 (2.95) | 2.91 (2.86) | 1.75 | 1.89 | 1.89 | |
| Methylated GC | | | | | | 2.79 | 2.93 | 2.91 | 1.76 | 1.90 | 1.89 | |
| GC' | | | | | | 2.81 | 2.92 | 2.91 | 1.78 | 1.89 | 1.89 | |
| GC'-1 | | | | | | 3.05 | 2.89 | 2.68 | 2.04 | 1.85 | | 1.67 |
| GC'-1$^*$ | | | | | | 3.03 | 2.89 | 2.68 | 2.01 | 1.85 | | 1.67 |
| GC'-2 | | | | | | 3.05 | 2.89 | 2.68 | 2.04 | 1.85 | | 1.67 |
| GC'-2$^*$ | | | | | | 3.05 | 2.89 | 2.68 | 2.04 | 1.85 | | 1.67 |
| GC'-3 | | | | | | 3.05 | 2.89 | 2.68 | 2.04 | 1.85 | | 1.67 |
| GC'-3$^*$ | | | | | | 3.05 | 2.89 | 2.68 | 2.04 | 1.85 | | 1.67 |

Data in parentheses denote the experimental data (Mo 2006; Saenger 1984).

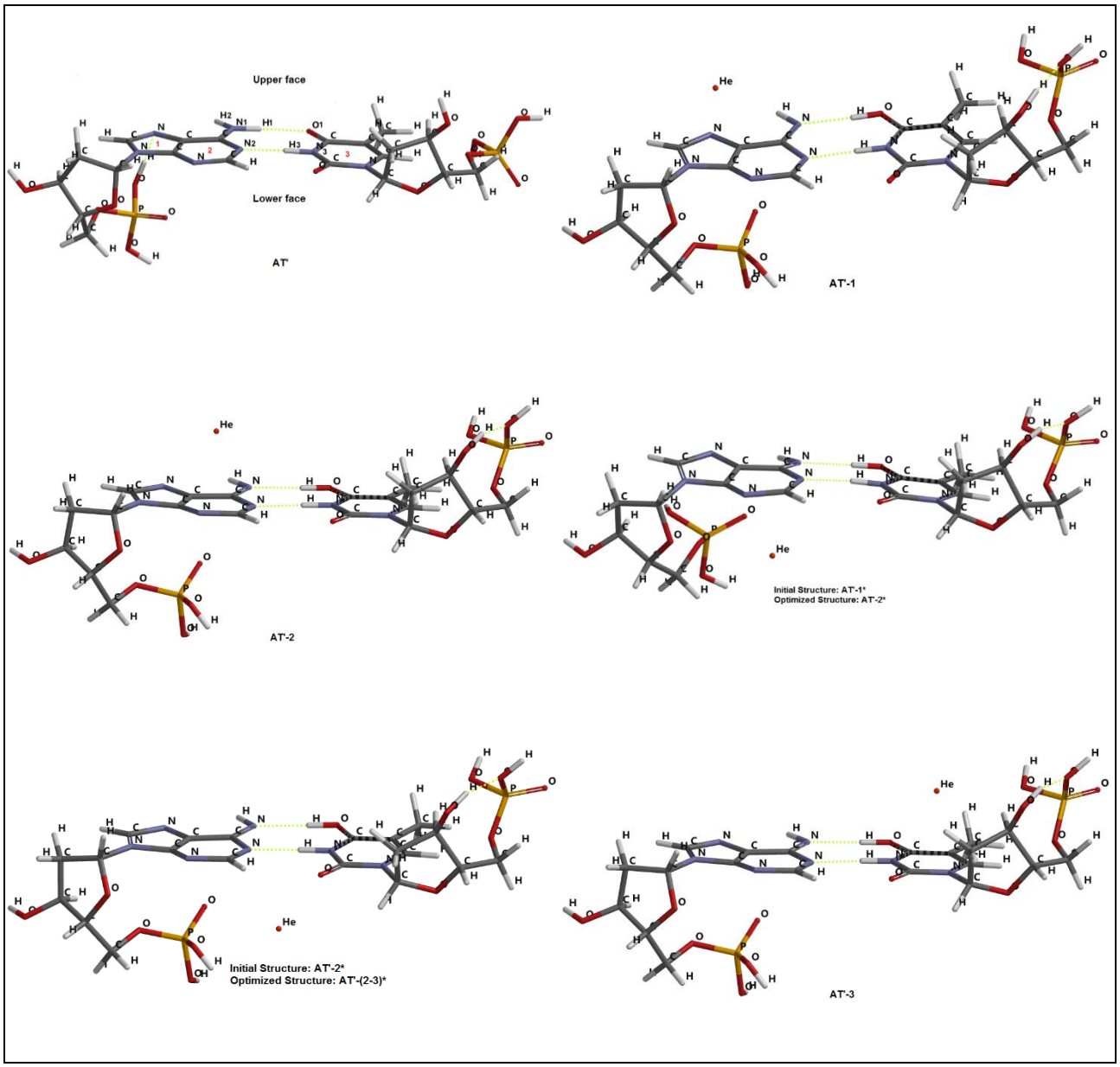


**Fig. 2** The optimized structures of AT' and GC' base pairs (with 2'-deoxyribose-5'-phosphate residues) and their $He^{2+}$ exposed derivatives at DFT UM06-2X/6-31G(d,p) theoretical level. The interactions of $He^{2+}$ from the upper faces of the base pairs were denoted as AT'-i and GC'-i (i=1-3), respectively, where i represented the aromatic ring numbers. Asterisk symbols ($^*$) over i, AT'-$i^*$ and GC'-$i^*$, were used to indicate the interactions from the lower face.

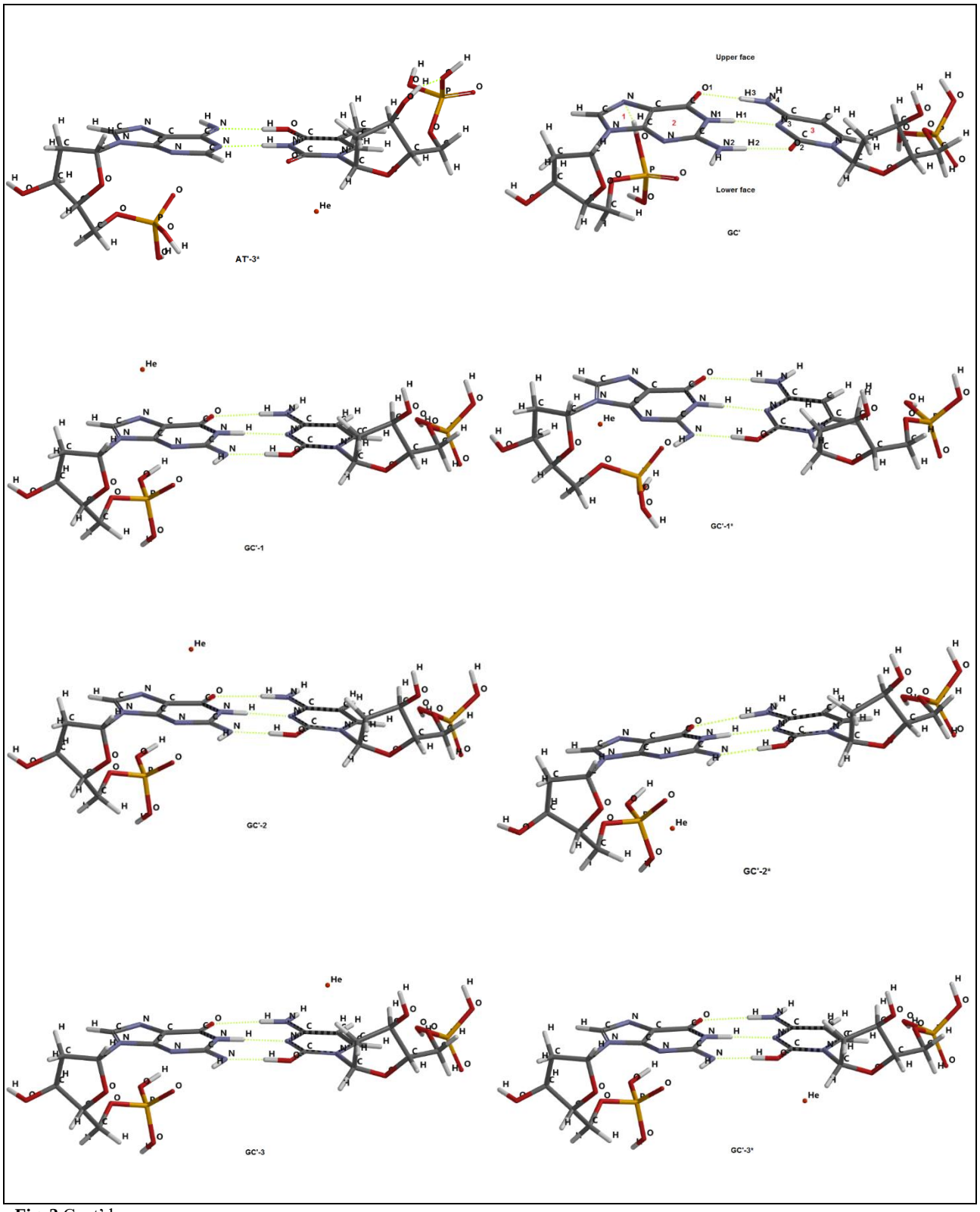


**Fig. 2** Cont'd.

which was located under Ring 2. Similarly, the $He^{2+}$ ion in AT'-2* initial structure shifted in between Rings 2 and 3 and formed the optimized structure of AT'-(2-3)*.

The hydrogen bonding atomic distances of the considered molecules were also demonstrated in Table 1. Compared to three molecules (AT, methylated AT and AT'), the $N_1$-$O_1$ distance slightly narrowed for most of the considered $He^{2+}$ exposed structures. It almost stayed the same for AT'-2*. The $H_1$-$O_1$ hydrogen bond turned into $N_1$-$H_1$ hydrogen bond by shift of $H_1$ from $N_1$ to $O_1$ in alpha radiated derivatives with almost no change in their bond distances (except for AT'-2*). The $N_2$-$N_3$ and relatedly $N_2$-$H_3$ distances of these base pairs increased compared to AT, methylated AT and AT'. The average elongation at $N_2$-$N_3$ distance was 0.06 Å whereas it was 0.08 Å at $N_2$-$H_3$ distance. It was possible to deduce that the hydrogen bond distances were affected when the AT' molecule was exposed to alpha radiation, i.e. the distance above narrowed, while that of the below elongated. However, the trend was opposite for the GC'-i and GC'-i* structures. The hydrogen bond distance above elongated whereas those of in the middle and below narrowed. This situation was explained as follows: The $O_1$-$N_4$ and corresponding $O_1$-$H_3$ distances increased significantly for alpha radiation exposed GC'-i and GC'-i* structures compared to GC, methylated GC and GC'. The average elongation at the $O_1$-$N_4$ distance was 0.25 Å whereas it was 0.28 Å at the $O_1$-$H_3$ distance. Conversely, the $N_1$-$N_3$ and corresponding $H_1$-$N_3$ distances narrowed slightly, i.e. average decreases of 0.03 Å and 0.04 Å were observed in the former and latter, respectively. Finally, the $N_2$-$O_2$ distance was reduced by 0.23 Å, forming a new, shorter hydrogen bond between the $N_2$ and $H_2$ atoms (1.67 Å in all) by the shift of $H_2$ from $N_2$ to $O_2$. Finally, it was figured out that more severe changes were observed in hydrogen bond distance in GC' rather than AT' when both of them were exposed to alpha radiation.

The interaction distance of $He^{2+}$ from the ring centres of alpha radiation exposed AT' and GC' specie was demonstrated in Table 2. The corresponding distances were detected between 2.68-2.82 Å for AT'-i and AT'-i* base pairs. Exceptionally, $He^{2+}$ lied somewhere in between adenine and thymine moieties of AT'-(2-3)* and located far away from the ring centres. Therefore, the larger distances were detected for it than for others (distances of 3.70 Å to Ring 2 and 4.10 Å to Ring 3). On the other hand, the related distances were obtained in between 2.69-3.56 Å for GC'-i and GC'-i* base pairs.

**Table 2.** The interaction distance of $He^{2+}$ (Å) from the ring centres of alpha radiation exposed AT' and GC' species optimized at DFT UM06-2X/6-31G(d,p) theoretical level.

| | Ring Number | | |
|---|---|---|---|
| Base Pair | 1 | 2 | 3 |
| AT'-1 | 2.76 | | |
| AT'-2 | | 2.68 | |
| AT'-2* | | 2.82 | |
| AT'-(2-3)* | | 3.70 | 4.10 |
| AT'-3 | | | 2.70 |
| AT'-3* | | | 2.69 |
| GC'-1 | 2.77 | | |
| GC'-1* | 3.35 | | |
| GC'-2 | | 2.71 | |
| GC'-2* | | 3.56 | |
| GC'-3 | | | 2.76 |
| GC'-3* | | | 2.69 |

### *3.3. Interaction Enthalpies and Gibbs Free Energies*

The interaction enthalpies and Gibbs free energies of the AT, GC, their methylated forms, AT', GC' and their alpha radiated derivatives were listed in Table 3. All the values listed in the table were negative which indicated favored interactions. In general, the interaction enthalpies presented more exothermic character than interaction Gibbs free energies. The first observation was that no dramatic changes were observed in both energies for un-radiated specie. However, the values became drastically more exothermic when AT' and GC' were exposed to alpha radiation. The interaction enthalpies changed between (-48.8)-(-62.8) kcal/mol and (-64.5)-(-93.8) kcal/mol for radiated AT' and GC' derivatives, respectively. On the other hand, the interaction Gibbs free energies changed between (-36.0)-(-52.1) kcal/mol and (-49.8)-(-79.9) kcal/mol for radiated AT' and GC' specie, respectively. Additionally, the energies of GC and its derivatives existing in the table were more exothermic than that of AT. This condition could be explained in terms of hydrogen bond numbers; i.e. the GC and its derivatives having three hydrogen bonds would have greater stability than that of AT having two hydrogen bonds. Another striking observation was that the AT' derivatives radiated from the thymine moieties (AT'-3 and AT'-3*) and similarly the GC' derivatives radiated from the cytosine moieties (GC'-3 and GC'-3*) showed more exothermic character than the others.

**Table 3.** The interaction enthalpies and Gibbs free energies of the specie listed in Table 1 (UM06-2X/6-311G(d)//UM06-2X/6-31G(d,p)).

| | $\Delta H^o_{298}$ (kcal/mol) | $\Delta G^o_{298}$ (kcal/mol) |
|---|---|---|
| AT | -14.1 | -2.6 |
| Methylated AT | -12.4 (-12.1) | -1.1 |
| AT' | -12.4 | -0.2 |
| AT'-1 | -51.0 | -37.6 |
| AT'-2 | -51.2 | -37.7 |
| AT'-2* | -48.8 | -36.0 |
| AT'-(2-3)* | -51.0 | -37.5 |
| AT'-3 | -62.8 | -52.0 |
| AT'-3* | -62.5 | -52.1 |
| GC | -27.4 | -15.4 |
| Methylated GC | -25.2 (-21.0) | -12.8 |
| GC' | -23.8 | -10.8 |
| GC'-1 | -65.1 | -51.5 |
| GC'-1* | -65.1 | -50.9 |
| GC'-2 | -65.0 | -51.4 |
| GC'-2* | -64.5 | -49.8 |
| GC'-3 | -93.8 | -79.9 |
| GC'-3* | -93.0 | -79.8 |

Energies are BSSE corrected. Data in parentheses denote the experimental data (Brameld et al. 1997; Guerra et al. 2000; Yanson et al. 1979).

### *3.4. Frontier Molecular Orbital (FMO) Analyses*

Mulliken electronegativity ($\chi_M$), electronic chemical potential (μ), absolute hardness (η), global softness (S) and electrophilicity index (ω) are important properties to understand the chemical reactivity of the compounds. They are obtained according to the Equations (1) - (4) below.

$$\chi_M = -\mu = (I + A) / 2 \quad (1)$$
(Pearson 1997; Srivastava et al. 2009)

$$\eta = (I - A) / 2 \quad (2)$$
(Pearson 1997; Singh et al. 2004)

$$S = 1 / (2\ \eta) \quad (3)$$
(Singh et al. 2004; Srivastava et al. 2009)

$$\omega = \mu^2 / (2\ \eta) \quad (4)$$
(Parr et al. 1999; Srivastava et al. 2009)

I and A are the ionization potential and electron affinity, respectively (Pearson 1997). Note that $I = -\varepsilon_{HOMO}$ and $A = -\varepsilon_{LUMO}$ within the validity of the Koopmans' theorem (Koopmans 1934), where $\varepsilon_{HOMO}$ and $\varepsilon_{LUMO}$ are the energies of the highest occupied molecular orbitals and lowest unoccupied molecular orbitals, respectively.

Electrophilicity index (ω) defines the global electrophilic nature of a molecule within a relative scale (Raya et al. 2011). If we consider two reacting molecules, the one having higher ω acts as an electrophile whereas the other with lower ω acts as a nucleophile. As expected, the radiated AT' and GC' derivatives had more electrophilic character than their unradiated forms (Table 4). The other point was that all the absolute hardness (η) and global softness (S) values were inversely proportional to each other for the considered species in the table. The unradiated base pairs, AT' and GC', were both harder than their radiated forms.

Molecules with high HOMO energy can donate their electrons more easily compared to molecules with low HOMO energy, and hence are more reactive in oxidation reactions. Accordingly, molecules with low LUMO energy are more apt to accept electrons than molecules with high LUMO energy. Hence, they are more reactive in reduction reactions. This information is used in describing the reactivity (stability) of the molecules. The $f_{H/L}$ index is defined as a stability index of molecules through oxidation. It's the ratio between the HOMO and LUMO energies. Molecules with low values of $f_{H/L}$ show more persistent character to oxidation than the molecules having high values of $f_{H/L}$ (Rokhina and Suri 2012). Accordingly, the AT' had lower $f_{H/L}$ value than GC' which denoted its more resistance to oxidation (Table 4).

Note that there was a strong relationship between the considered AT' and GC' base pairs' oxidation tendency and their radiation interaction energies. The higher $f_{H/L}$ value of GC' indicated that it was more prone to oxidation and as a result the radiated derivatives of it showed more exothermic interaction energies than that of AT'. Additionally, the $f_{H/L}$ values of all the radiated specie lied in between that of AT' and GC'.

## 4. Conclusion

It is known that the theoretical method and basis set used in such computational studies act as limiting parameters for the obtained results. However, in the present study, the selection of these two was mainly based on comparison of the results with experimental data as much as possible. In the light of this, the major outcomes of the study were summarized as follows:

a. When the AT' and GC' base pairs (Adenine-Thymine and Guanine-Cytosine base pairs including 2'-deoxyribose-5'-phosphate residues) were exposed to alpha radiation, the hydrogen bond distances were severely affected. The distance above narrowed while that of the below elongated in all the radiated AT'

**Table 4.** The frontier molecular orbital energies, reactivities and stabilities of AT', GC' and their $He^{2+}$ exposed derivatives (UM06-2X/6-311G(d)//UM06-2X/6-31G(d,p)).

| | $\varepsilon_{HOMO}$ (eV) | $\varepsilon_{LUMO}$ (eV) | I (eV) | A (eV) | $\chi_M$ (eV) | $\eta$ (eV) | S ($eV^{-1}$) | $\omega$ (eV) | $f_{H/L}$ |
|---|---|---|---|---|---|---|---|---|---|
| AT' | -0.27 | 0.0067 | 0.27 | -0.0067 | 0.13 | 0.14 | 3.6 | 0.06 | -40.3 |
| AT'-1 | -0.48 | -0.37 | 0.48 | 0.37 | 0.43 | 0.06 | 9.1 | 1.6 | 1.3 |
| AT'-2 | -0.48 | -0.37 | 0.48 | 0.37 | 0.43 | 0.06 | 9.1 | 1.6 | 1.3 |
| AT'-2* | -0.48 | -0.38 | 0.48 | 0.38 | 0.43 | 0.05 | 10.0 | 1.8 | 1.3 |
| AT'-(2-3)* | -0.48 | -0.37 | 0.48 | 0.37 | 0.43 | 0.06 | 9.1 | 1.6 | 1.3 |
| AT'-3 | -0.48 | -0.37 | 0.48 | 0.37 | 0.43 | 0.06 | 9.1 | 1.6 | 1.3 |
| AT'-3* | -0.48 | -0.37 | 0.48 | 0.37 | 0.43 | 0.06 | 9.1 | 1.6 | 1.3 |
| GC' | -0.24 | -0.00021 | 0.24 | 0.00021 | 0.12 | 0.12 | 4.2 | 0.06 | 1142.9 |
| GC'-1 | -0.50 | -0.36 | 0.50 | 0.36 | 0.43 | 0.07 | 7.1 | 1.3 | 1.4 |
| GC'-1* | -0.50 | -0.36 | 0.50 | 0.36 | 0.43 | 0.07 | 7.1 | 1.3 | 1.4 |
| GC'-2 | -0.50 | -0.36 | 0.50 | 0.36 | 0.43 | 0.07 | 7.1 | 1.3 | 1.4 |
| GC'-2* | -0.50 | -0.36 | 0.50 | 0.36 | 0.43 | 0.07 | 7.1 | 1.3 | 1.4 |
| GC'-3 | -0.50 | -0.36 | 0.50 | 0.36 | 0.43 | 0.07 | 7.1 | 1.3 | 1.4 |
| GC'-3* | -0.50 | -0.36 | 0.50 | 0.36 | 0.43 | 0.07 | 7.1 | 1.3 | 1.4 |

derivatives. However, the trend was opposite for the radiated GC' structures, i.e. the bond distances above elongated whereas those of in the middle and below narrowed. However, more drastic changes were observed in radiated GC' specie rather than AT' specie in terms of hydrogen bond distance.

b. The alpha radiation interaction energy values of AT' and GC' were negative (exothermic). Additionally, the interaction enthalpies presented more exothermic character than interaction Gibbs free energies. However, the AT' derivatives radiated from the thymine moieties and the GC' derivatives radiated from the cytosine moieties presented more exothermic character than the others.

c. The higher $f_{H/L}$ value of GC' revealed that it was more favoured to be oxidized by $He^{2+}$ than AT' and consequently the $He^{2+}$ complexes of GC' had more exothermic interaction energies (formed more spontaneously) than that of AT'.

**Acknowledgements**

Thanks to Zonguldak Bulent Ecevit University Scientific Research Projects Coordination Office for financial support (Project No. BAP-2020-77654622-03).

**Authors' Contributions**

The author contributed to each part of the study.

**Conflict of Interest Disclosure**

The author reports no conflicts of interest.

**References**

Bale WF. 1980. Memorandum to the files, March 14, 1951: hazards associated with radon and thoron. Health Phys. 38(6):1062-1066.

Boys SF, Bernardi F. 1970. The calculation of small molecular interactions by the differences of separate total energies. Some procedures with reduced errors. Mol. Phys. 19(4):553-566.

Brameld K, Dasgupta S, Goddard WA. 1997. Distance dependent hydrogen bond potentials for nucleic acid base pairs from ab initio quantum mechanical calculations (LMP2/cc-pVTZ). J. Phys. Chem. B 101(24):4851-4859.

Chen DJ, Strniste GF, Tokita N. 1984. The genotoxicity of alpha particles in human embryonic skin fibroblasts. Radiat. Res. 100(2):321-327.

Davis MR, Dougherty DA. 2015. Cation-π interactions: computational analyses of the aromatic box motif and the fluorination strategy for experimental evaluation. Phys. Chem. Chem. Phys. 17(43):29262-29270.

Dhindhwal V, Sathyamurthy N. 2016. The effect of hydration on the cation-π interaction between benzene and various cations. J. Chem. Sci. 128(10):1597-1606.

Durrani SA, Ilić R. 1997. Radon measurements by etched track detectors: applications in radiation protection, earth sciences and the environment. World Scientific, Singapore, New Jersey, London, Hong Kong.

Ebrahimi A, Karimi P, Akher FB, Behazin R, Mostafavi N. 2014. Investigation of the π-π stacking interactions without direct electrostatic effects of substituents: the aromatic‖aromatic and aromatic‖anti-aromatic complexes. Mol. Phys. 112(7):1047-1056.

Guerra CF, Bickelhaupt FM, Snijders JG, Baerends EJ. 2000. Hydrogen bonding in DNA base pairs: reconciliation of theory and experiment. J. Am. Chem. Soc. 122(17):4117-4128.

Harley JH. 1952. Sampling and measurement of airborne daughter products of radon [dissertation]. Rensselaer Polytechnic Institute, Troy (NY).

Hollstein M, Bartsch H, Wesch H, Kure EH, Mustonen R, Mühlbauer KR, Spiethoff A, Wegener K, Wiethege T, Müller KM. 1997. p53 gene mutation analysis in tumors of patients exposed to alpha-particles. Carcinogenesis 18(3):511-516.

Koopmans T. 1934. Über die zuordnung von wellenfunktionen und eigenwerten zu den einzelnen elektronen eines atoms. Physica 1(1-6):104-113.

McDonald JW, Taylor JA, Watson MA, Saccomanno G, Devereux TR. 1995. p53 and K-ras in radon-associated lung adenocarcinoma. Cancer Epidemiol., Biomarkers Prev. 4(7):791-793.

Mo, Y. 2006. Probing the nature of hydrogen bonds in DNA base pairs. J. Mol. Model. 12(5):665-672.

Mottishaw JD, Sun H. 2013. Effects of aromatic trifluoromethylation, fluorination, and methylation on intermolecular π-π interactions. J. Phys. Chem. A 117(33):7970-7979.

Mudedla SK, Balamurugan K, Subramanian V. 2014. Computational study on the interaction of modified nucleobases with graphene and doped graphenes. J. Phys. Chem. C 118(29):16165-16174.

Narayanan PK, Goodwin EH, Lehnert BE. 1997. Alpha particles initiate biological production of superoxide anions and hydrogen peroxide in human cells. Cancer Res. 57(18):3963-3971.

National Radiological Protection Board. 1998. Living with radiation. NRPB, London.

Parr RG, Szentpály LV, Liu S. 1999. Electrophilicity index. J. Am. Chem. Soc. 121(9):1922-1924.

Pearson RG. 1997. Chemical hardness. Wiley-VCH, Weinheim, New York (NY).

Popp W, Vahrenholz C, Schuster H, Wiesner B, Bauer P, Täuscher F, Plogmann H, Morgenroth K, Konietzko N, Norpoth K. 1999. p53 mutations and codon 213 polymorphism of p53 in lung cancers of former uranium miners. J. Cancer Res. Clin. Oncol. 125(5):309-312.

Raya A, Barrientos-Salcedo C, Rubio-Póo C, Soriano-Correa C. 2011. Electronic structure evaluation through quantum chemical descriptors of 17β-aminoestrogens with an anticoagulant effect. Eur. J. Med. Chem. 46(6):2463-2468.

Robertson A, Allen J, Laney R, Curnow A. 2013. The cellular and molecular carcinogenic effects of radon exposure: a review. Int. J. Mol. Sci. 14(7):14024-14063.

Rokhina EV, Suri RPS. 2012. Application of density functional theory (DFT) to study the properties and degradation of natural estrogen hormones with chemical oxidizers. Sci. Total Environ. 417-418:280-290.

Saenger W. 1984. Principles of nucleic acid structure. Springer-Verlag, New York (NY).

Singh PP, Srivastava HK, Pasha FA. 2004. DFT-based QSAR study of testosterone and its derivatives. Bioorg. Med. Chem. 12(1):171-177.

Soğukpınar H. 2013. Determination of seasonal correction factors for indoor radon concentrations in Eskisehir [dissertation]. Eskişehir Osmangazi University, Eskişehir, Turkey.

Spartan'18 Parallel Suite. 2018. Wavefunction, Inc., Irvine (CA).

Srivastava HK, Pasha FA, Mishra SK, Singh PP. 2009. Novel applications of atomic softness and QSAR study of testosterone derivatives. Med. Chem. Res. 18(6):455-466.

Taylor JA, Watson MA, Devereux TR, Michels RY, Saccomanno G, Anderson M. 1994. p53 mutation hotspot in radon-associated lung cancer. Lancet 343(8889):86-87.

Wazer DE, Chu Q, Liu XL, Gao Q, Safaii H, Band V. 1994. Loss of p53 protein during radiation transformation of primary human mammary epithelial cells. Mol. Cell. Biol. 14(4):2468-2478.

Wesch H, Wiethege T, Spiethoff A, Wegener K, Müller KM, Mehlhorn J. 1999. German uranium miner study: historical background and available histopathological material. Radiat. Res. 152(6s):S48-S51.

Wiethege T, Wesch H, Wegener K, Müller KM, Mehlhorn J, Spiethoff A, Schömig D, Hollstein M, Bartsch H. 1999. German uranium miner study: pathological and molecular genetic findings. Radiat. Res. 152(6s):S52-S55.

Yang Q, Wesch H, Mueller KM, Bartsch H, Wegener K, Hollstein M. 2000. Analysis of radon-associated squamous cell carcinomas of the lung for a p53 gene hotspot mutation. Br. J. Cancer 82(4):763-766.

Yanson IK, Teplitsky AB, Sukhodub LF. 1979. Experimental studies of molecular interactions between nitrogen bases of nucleic acids. Biopolymers 18(5):1149-1170.

Zeeb H, Shannoun F. 2009. WHO handbook on indoor radon: a public health perspective. World Health Organization, France.

Zhao Y, Truhlar DG. 2008. Density functionals with broad applicability in chemistry. Acc. Chem. Res. 41(2):157-167